ISBN: 978-3-95450-184-7 doi:10.18429/JACoW-IPAC2018-THPAK002

UPDATED MODEL OF THE RESISTIVE WALL IMPEDANCE FOR THE MAIN RING OF J-PARC

B. Yee-Rendon*, Y.H. Chin, H. Kuboki and T. Toyama
KEK/J-PARC, Tsukuba, Ibaraki, Japan
M. Schenk, CERN, Geneva, Switzerland

Abstract

The resistive wall impedance is one of the major contributors of the impedance in the Main Ring of J-PARC. The present model assumes round chambers of stainless steel with perfect magnet boundary conditions for its surroundings. This work presents the model of the resistive wall impedances taking into account the different chamber geometries of Main Ring, the materials and more realistic surroundings. The models were benchmarked with measurements of the coherent tune shift of the Main Ring of J-PARC. The simulation of beam instabilities is a helpful tool to evaluate potential threats against the machine protection of the high intensity beams.

INTRODUCTION

The Main Ring is the last step in the accelerator chain of J-PARC. It is a synchrotron machine that accelerates protons from an energy of 3 to 30 GeV for the Hadron and Neutrino experimental facilities [1]. Main Ring has a three fold symmetry with a length of 1567.5 m. At the beginning, the beam pipe was made entirely of stainless steel (St St), however, a fraction of the ducts were replaced with titanium (Ti) from October 2013 to January 2014 [2]. In this accelerator, the resistive wall impedance is one of the dominant sources for beam instabilities, thus, its precise evaluation and beam interaction are important for the good performance of the machine. The impedance budget, in particular the resistive wall, is benchmarked with beam measurements to test its validity. In this work the resistive wall and the so-called wall impedance (resistive wall plus the indirect space charge) [3] were computed and compared against the coherent tune shift measurements done in December 2015, the results of that survey are presented in Table 1.

Table 1: Coherent tune shifts measurements for a single bunch at J-PARC Main Ring. The beam energy was 3 GeV, the unperturbed horizontal tune Q_{xo} was 22.41, the vertical tune Q_{yo} was 20.774 and the chromaticity ξ was -5.

Intensity [10^{12} **p**]	**Bunch length** (σ_l) [m]	ΔQ_x [10^{-3}]	ΔQ_y [10^{-3}]
4.26 ± 0.02	12.17 ± 0.58	-0.9 ± 3.0	-6.4 ± 18.0
8.50 ± 0.05	12.40 ± 0.58	-3.5 ± 1.0	-8.3 ± 2.5
12.60 ± 0.08	13.16 ± 0.58	-5.6 ± 1.5	-10.5 ± 1.0
16.80 ± 0.10	13.86 ± 0.58	-6.4 ± 2.0	-14.1 ± 1.3
19.30 ± 0.20	13.83 ± 0.58	-7.6 ± 2.5	-16.1 ± 1.3

* byee@post.j-parc.jp

IMPEDANCE MODEL

The previous resistive wall impedance scheme consisted of round chambers with one single layer of St St with perfect magnet boundary (model A) [4]. In that case the impedance was generated according to the formalism of Zotter-Metral [5, 6] using

$$Z_\perp(f) = \frac{jLZ_o I_1^2(s)K_1(x_1)}{\pi a^2 \beta\gamma^2 I_1(x_1)} \times \frac{\gamma v(P_1 - Q_1)(\beta x_1 x_2)^2(\gamma v P_1 - k\mu' Q_\eta)}{(\gamma v x_2 - k x_1)^2 - (\beta x_1 x_2)^2(\gamma v P_1 - k\mu' Q_\eta)(\gamma v P_1 - k\epsilon' Q_\alpha)} \quad (1)$$

The complete description of the variables in Eq. 1 can be found in reference [6]. For model A, the St St chamber has a DC resistivity of 740 nΩ–m, radius of 65 mm, thickness of the layer 2 mm, energy 3 GeV and a perfect magnet boundary.

Since the Main Ring chamber shapes are more complex than only circular geometry, the code Impedance Wake 2D (IW2D) was used. IW2D has the advantages to compute transverse and longitudinal beam coupling impedances and wake fields for multilayer structures, cylindric and flat shapes [7].

Model B was composed of two layers of round chambers: the first layer of St St with a thickness of 2 mm, the second one was an infinitely thick layer of silicon-steel. This last configuration was defined to simulate the boundary conditions of the beam pipe surroundings by the magnets (dipoles and quadrupoles) and it was implemented through

$$\mu_r(f) = \frac{1 + \mu_m}{1 + jf/f_\mu} \quad (2)$$

where μ_m is the magnetic susceptibility which was 500, f_μ the relaxation frequency of permeability was 10 MHz and f is the frequency.

Model C divides the ring into two simple geometries: sixty five percent of round shapes to describe the straight section and thirty five percent elliptical for the bending regions. The radius of the circular section is the same value of 65 mm and for the elliptical ones the height is 100 mm and the width is 131 mm. The same material, thickness and boundary conditions as for model B were assumed.

Finally, the scheme D is similar as C, with the only difference that this one takes into account the different materials of the beam pipes: two third of St St and one third of Ti with a DC resistivity of 430 nΩ–m. Figure 1 presents the horizontal dipolar components of the four models.

ISBN: 978-3-95450-184-7 doi:10.18429/JACoW-IPAC2018-THPAK002

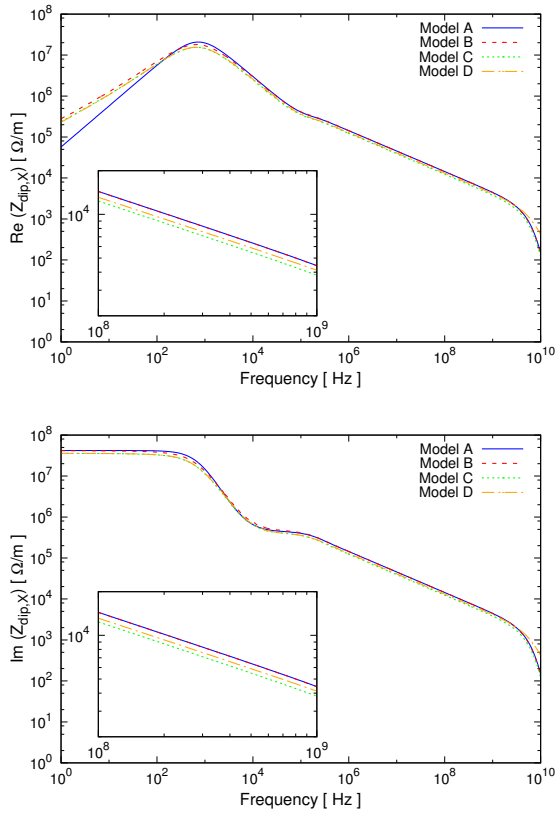

Figure 1: Horizontal dipolar impedance for the four models (real part on the top, imaginary part on the bottom).

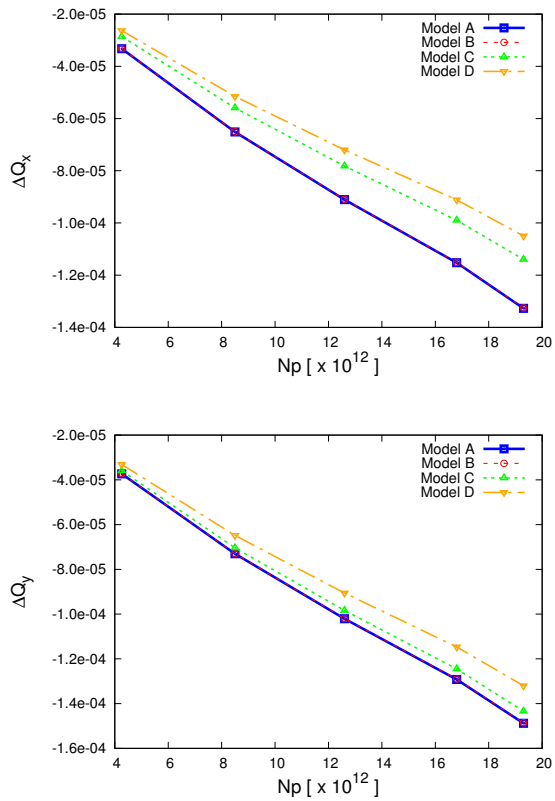

Figure 2: The resistive wall coherent tune shifts produced by the four models (horizontal on the left part, vertical on the right part). These plots show a $\Delta Q_{\mathrm{RW}} \approx 10^{-4} \sim 10^{-5}$ which is smaller than $\Delta Q_{\mathrm{Meas.}} \approx 10^{-2} \sim 10^{-3}$ computed from data of Table 1.

TUNE SHIFT BENCHMARK

The coherent tune shift for a Gaussian beam is computed using

$$\begin{aligned}\Delta Q^{(l)} &= \frac{1}{\omega_o}\Re(\Omega^l - \omega_\beta - l\omega_s) \\ &= \frac{1}{\omega_o}\Re(\frac{1}{4\sqrt{\pi}}\frac{\Gamma(l+\frac{1}{2})}{2^l l!}\frac{Nr_o c^2}{\gamma T_o \omega_\beta \sigma} i(Z_{\mathrm{eff}}))\end{aligned} \tag{3}$$

where Z_{eff} is defined as

$$Z_{\mathrm{eff}} = \frac{\sum_{p=-\infty}^{\infty} Z(\omega') h_l(\omega' - \omega_\xi)}{\sum_{p=-\infty}^{\infty} h_l(\omega' - \omega_\xi)} \tag{4}$$

with Z the impedance, $h_l(\omega) = (\frac{\omega\sigma}{c})^{2l}\exp(-\frac{\omega^2\sigma^2}{c^2})$, $\omega' = \omega_o p + \omega_\beta$, the definition of the remains variables in Eqs. 3 and 4 can be found in reference [8]. The coherent tune shifts calculated by Eq. 3 were only for mode zero for the four models of resistive wall impedance. The results are shown in Fig. 2.

In addition, the coherent tune shifts generated for the indirect space charge were calculated by the following formula

$$\Delta Q_{x/y} = -\frac{Nr_o R}{\pi\gamma\beta^2 Q_{x/yo}}[\frac{1-\chi_e-\beta^2}{B}\frac{\xi_1^{x/y}}{h^2} + \frac{\beta^2\epsilon_1^{x/y}}{h^2}] \tag{5}$$

The complete description of the variables in Eq. 5 can be found in reference [9]. Model A has the same values as B and model C and D are equal (see Table 2).

Table 2: Coherent Tune Shifts Computed using the Laslett Coefficients.

Intensity [10^{12} **p**]	**Model A & B** $\Delta Q_{x/y}$ [10^{-2}]	**Model C & D** $\Delta Q_{x/y}$ [10^{-2}]
4.2	-0.49/-0.53	-0.46/-0.71
8.5	-0.97/-1.05	-0.91/-1.40
12.6	-1.36/-1.47	-1.27/-1.97
16.8	-1.73/-1.86	-1.61/-2.49
19.3	-1.99/-2.15	-1.85/-2.87

Combining both results of resistive wall (Fig. 2) and indirect space charge (Table 2), the tune shift due to the wall impedance was estimated. That result is compared against the measurement of the coherent tune shifts of the J-PARC Main Ring in Fig. 3.

ISBN: 978-3-95450-184-7 doi:10.18429/JACoW-IPAC2018-THPAK002

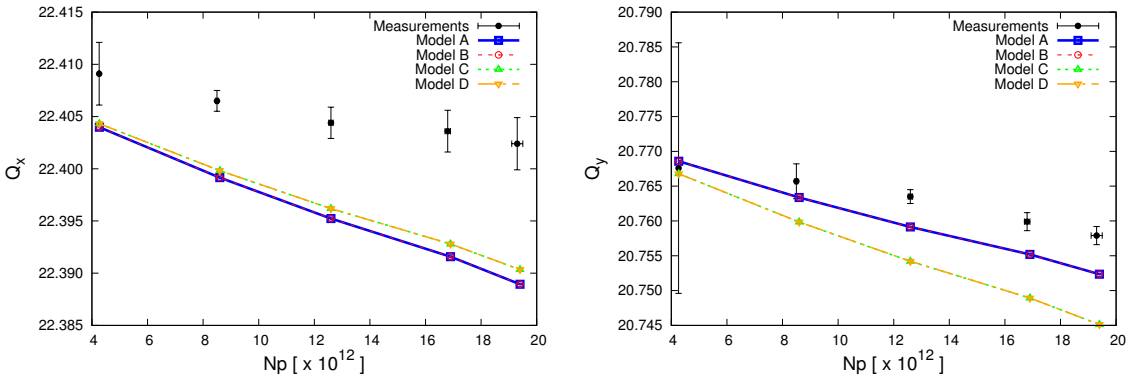

Figure 3: The tune produced by the wall impedance (indirect space charge plus resistive wall): horizontal (left) and vertical (right). The calculations overestimate the measurements.

CONCLUSIONS

Four different models of the resistive wall impedance for the J-PARC Main Ring were computed using the Zotter-Metral formula or the impedance code IW2D. The impedances generated were benchmarked against the coherent tune shift measurements for a single bunch. Additionally, the indirect space charge was calculated to estimate the wall impedance (resistive wall plus indirect space charge) coherent tune shifts. The cases of round chambers made of stainless steel : models A (a single layer plus perfect magnet boundary using the analytical equation) and B (double layers plus silicon-steel boundary using the impedance code). Both schemes produced the same results shown in Figs. 1 to 3. This indicates that perfect magnetic boundary is a good approximation to describe the beam pipe surroundings for the Main Ring. Models C (sixty five percent round chambers, thirty five percent elliptical chambers, stainless steel) and D (same chamber shape configuration as case C, moreover, two third stainless steel one third titanium) both generated by IW2D. For these schemes, the last one produced the smallest tune shifts. This can be explained due to the fact that titanium has a smaller DC resistivity than stainless steel.

Figure 2 shows that the resistive wall by itself can not reproduce the measurements of coherent tune shifts. In contrast, the wall impedance overestimates them (Fig. 3). The wall impedance of the four models produced similar horizontal tune shifts, on the contrary, the vertical tune shifts are larger for the cases C and D than A and B. These results are justified by the horizontal and vertical half apertures in the schemes: models A and B $hx/y = 6.55$ cm, models C and D $hx = 6.55$ cm and $hy = 5.00$ cm. The resistive wall results indicated: 1) The relevance of the indirect space charge at injection energy; 2) The overestimation can be attributed to the fact that the kicker impedance (which is another important source of the impedance at the Main Ring) was not taken into account for this calculation.

The present resistive wall scheme (model D) provides a more accurate description of the actual Main Ring resistive wall than the previous version (model A). However, the resistive wall itself is insufficient to reproduce the coherent tune shift measurements. Thus, future work will include for one side an improvement of the resistive wall model by computing more realistic chamber geometries, surroundings and on other hand by adding the impedance contribution of more elements such as the injection and extraction kickers.

ACKNOWLEDGMENT

The authors thank N. Biancacci, N. Mounent, B. Salvant, Y. Shobuda and M. Uota for the fruitful discussions. This work was partially supported by JSPS KAKENHI Grant Number JP16H06288.

REFERENCES

[1] Accelerator Group JAERI/KEK Joint Project Team et al., "Accelerator Technical Design Report for J-PARC", JAERI-Tech 2003-044, KEK Report 2002-13 (2003).

[2] M. Uota et al., "Vacuum Ducts Modification to Shape and Material in J-PARC MR", in Proc. 12th Annual Meeting of Particle Accelerator Society of Japan, Tsuruga, Japan, August 2015, pp. 1342-1346 (In Japanese).

[3] F. Roncarolo et al,"Comparison between laboratory measurements, simulations, and analytical predictions of the transverse wall impedance at low frequencies", Phys. Rev. ST AB **12**, 084401,2009, doi: 10.1103/PhysRevSTAB.12.084401

[4] Y.H. Chin et al., "Impedance and Beam Instability Issues at J-PARC Rings", in Proc. of the Hadron Beam Conference, Nashville, U.S.A., August 2008, pp. 40-44.

[5] B. Zotter,"New Results on the Impedance of Resistive Metal Walls of Finite Thickness", Rep. CERN-AB-2005-043, 2005.

[6] E. Metral,"Transverse Resistive-Wall Impedance From Very Low to Very High Frequencies", Rep. CERN-AB-2005-084, 2005.

[7] N. Mounent, "The LHC Transverse Coupled-Bunch Instability", PhD thesis, Lausanne, EPFL, March 2012; Rep. CERN-BE-2009-039,2009.

[8] A.W. Chao, "Physics of collective beam instabilities in high energy accelerator", Ed. New York, NY, USA: Wiley, 1993.

[9] K.Y. Ng, "Betatron Tune Shifts and Laslett Image Coefficient", Rep. FERMILAB-TM-2152, 2001.